Structure, magnetic ordering, and spin filtering efficiency of NiFe2O4(111) ultrathin films

S. Matzen, J.-B. Moussy, P. Wei, Christophe Gatel, J. C. Cezar, M. A. Arrio, Ph. Sainctavit, J. S. Moodera

Structure, magnetic ordering, and spin filtering efficiency of $NiFe_2O_4$(111) ultrathin films

S. Matzen, J.-B. Moussy, P. Wei, C. Gatel, J. C. Cezar, M. A. Arrio, Ph. Sainctavit, and J. S. Moodera

Citation: Appl. Phys. Lett. **104**, 182404 (2014); doi: 10.1063/1.4871733
View online: https://doi.org/10.1063/1.4871733
View Table of Contents: http://aip.scitation.org/toc/apl/104/18
Published by the American Institute of Physics

Structure, magnetic ordering, and spin filtering efficiency of $NiFe_2O_4(111)$ ultrathin films

S. Matzen,[1,a)] J.-B. Moussy,[1,b)] P. Wei,[2] C. Gatel,[3] J. C. Cezar,[4,c)] M. A. Arrio,[5] Ph. Sainctavit,[5] and J. S. Moodera[2,6]
[1]*CEA, IRAMIS, SPCSI, F-91191 Gif-sur-Yvette, France*
[2]*Francis Bitter Magnet Laboratory, Massachusetts Institute of Technology, Cambridge, Massachusetts 02139, USA*
[3]*CEMES-CNRS, F-31055 Toulouse, France*
[4]*ESRF, F-38043 Grenoble, France*
[5]*IMPMC, F-75015 Paris, France*
[6]*Physics Department, Massachusetts Institute of Technology, Cambridge, Massachusetts 02139, USA*

(Received 20 November 2013; accepted 7 April 2014; published online 6 May 2014)

$NiFe_2O_4(111)$ ultrathin films (3–5 nm) have been grown by oxygen-assisted molecular beam epitaxy and integrated as effective spin-filter barriers. Structural and magnetic characterizations have been performed in order to investigate the presence of defects that could limit the spin filtering efficiency. These analyses have revealed the full strain relaxation of the layers with a cationic order in agreement with the inverse spinel structure but also the presence of antiphase boundaries. A spin-polarization up to +25% has been directly measured by the Meservey-Tedrow technique in $Pt(111)/NiFe_2O_4(111)/\gamma\text{-}Al_2O_3(111)/Al$ tunnel junctions. The unexpected positive sign and relatively small value of the spin-polarization are discussed, in comparison with predictions and previous indirect tunnelling magnetoresistance measurements. © *2014 AIP Publishing LLC*. [http://dx.doi.org/10.1063/1.4871733]

In spintronics, the capability of generating highly spin-polarized electron currents is critical for the optimal operation of spin-based devices. Different approaches are being investigated, with recent focus on the transport mechanism of spin-polarized electrons through a tunnel barrier. Spin filtering approach is particularly interesting in order to overcome the problem of efficient spin injection into semiconductors. Very high current spin-polarization (SP) can be generated by wave-function symmetry filtering when using epitaxial tunnel barriers. Tunneling magnetoresistance (TMR) values of several hundreds of percents have been achieved by this technique in magnetic tunnel junctions (MTJs) composed of ferromagnetic electrodes (used as spin-polarized electron sources) and a MgO tunnel barrier.[1,2] Another approach that has been little explored is the spin filtering through a ferro- or ferrimagnetic tunnel barrier.[3] Here, because the barrier is both insulating and magnetic, there is an exchange splitting of its conduction band, allowing creating two distinct tunnel barrier heights for spin-up and spin-down electrons, leading to the spin-selective transport of electrons. A large SP can thus result from the spin filtering through the magnetic insulator, using any usual metallic electrodes as non-polarized electron sources. Spin-filters barriers could then be integrated in future generations of spintronic devices since they may function with 100% efficiency[4] and at room temperature[5,6] if using ferromagnetic insulating materials with high Curie temperature (T_c), such as ferrites.[7] A few studies have been performed on these materials ($NiFe_2O_4$ (NFO),[8,9] $CoFe_2O_4$ (CFO),[5,6,10,11] and $MnFe_2O_4$[12] spin-filters), but they all reported relatively small SP values (~25% maximum), often limited to a low temperature range, while room temperature spin filtering[5,6] has only been obtained in $CoFe_2O_4$-based junctions showing a SP value of −8%.[6]

The spin filtering efficiency is governed by spin-dependent tunneling transport mechanisms through the magnetic insulating ultrathin film, and is thus affected by the band structure of the material and the presence of defects. Only few results have been obtained in ferrites spin-filters due to the difficulty of fabricating these complex oxides in ultrathin films with high structural and physical properties. Moreover, the few spin-polarized transport measurements were rarely directly related to a detailed structural and chemical characterization of the ultrathin films.[6,10,12] Understanding the observed limitations of spin filtering efficiency in ferrites barriers appears thus particularly crucial both from a fundamental and from a technological standpoint.

In this Letter, we present spin-polarized transport experiments through NFO tunnel barriers, together with a detailed characterization of the ultrathin films, mainly focused on usual defects in ferrites thin films (antiphase boundaries (APBs), cationic disorder, and oxygen vacancies). Among the ferrites, the benefit of NFO is due to its highest T_c (~850 K), good insulating behavior (band gap ~1 eV), and large exchange splitting of the conduction band (~1.2 eV). Up to now, CFO has been more studied as spin-filter barriers[5,6,10,11] and the presence of oxygen vacancies[10] or APBs[6] have both been recently shown to decrease the spin filtering efficiency. For NFO, much less is known. The few results published on NFO barriers were only obtained by TMR measurements,[8,9] using a ferromagnetic layer as spin analyzer whose SP has to be known. These studies raised the issue of the sign of SP values[9] but they lacked information on the structural and chemical qualities of the films used for these experiments, which are really crucial to understand their spin filtering capabilities.

[a)]Now at Univ. Paris 11, CNRS, UMR 8622, IEF, F-91405 Orsay, France.
[b)]Author to whom correspondence should be addressed. Electronic mail: jean-baptiste.moussy@cea.fr.
[c)]Now at CNPEM/LNLS, Campinas, Brazil.

In this work, we investigate the presence of structural and chemical defects in NFO tunnel barriers and we measure directly their spin filtering efficiency by the Meservey-Tedrow technique. These measurements give complementary information on the spin-polarized tunneling mechanism through NFO barriers, thanks to the direct determination of the spin-polarization of the tunneling current using a superconducting aluminum electrode as the spin detector, performed at lower bias than in TMR measurements, so closer to the direct tunneling mechanism.

NFO(111) layers were grown by oxygen-assisted molecular beam epitaxy (O-MBE) on α-Al_2O_3(0001) substrates or Pt(111) underlayers, following a procedure inspired by the optimized growth of $CoFe_2O_4$(111).[13] The samples were fabricated using different oxygen partial pressures (P_{O2}), ranging from $P_{O2} = 0.24$ to 0.40 Torr, to investigate the effect of oxygen vacancies on the spin filtering capability of NFO ultrathin films. Figure 1(a) shows a high resolution transmission electron microscopy (HRTEM) micrograph of the NFO(111) ultrathin film. The epitaxial relationship can be expressed as NFO(111)[-110]//α-Al_2O_3(0001)[-1100]. The geometric phase analysis (GPA) method was used to access the local deformations and strain fields in the NFO layers. On α-Al_2O_3(0001) substrate (in-plane lattice parameter of 0.476 nm), the strong in-plane lattice mismatch between NFO (cubic lattice parameter of 0.8331 nm) and the substrate reaches 8% (substrate taken as reference). We measured the in-plane (ε_{xx}) and out-of-plane (ε_{yy}) deformations of the NFO layer taking the reference within the substrate far from the interface. These deformations correspond to the variation of the interreticular distances (g_{hkl}) with the α-Al_2O_3 ones. In Figs 1(b) and 1(c) are reported the strain field analyses in the NFO layer based on the HRTEM image on top. Fig. 1(b) presents the in-plane deformation map comparing g_{-440} for NFO and g_{-3300} for α-Al_2O_3. The experimental value of $\varepsilon_{xx} = 8\% \pm 1\%$ is close to the theoretical deformation (7.2%) due to the mismatch. In the case of a perfect strained layer, the measured value should be close to 0%. We applied the same method in Fig. 1(c) to obtain the out-of-plane deformation map using g_{111} for NFO and g_{0003} for α-Al_2O_3. The deformation of $\varepsilon_{yy} = 10.5\% \pm 1\%$ remains close to the theoretical one (11.08%). Consequently, this analysis demonstrates the full strain relaxation of the NFO layer accompanied by misfit dislocations visible on the HRTEM micrograph. This analysis also reveals the presence of APBs in the ultrathin films, surrounding structural domains with lateral sizes around 20–30 nm. This result is consistent with the recent observation of APBs in 200 nm-thick NFO films.[14] APBs are well-known structural defects in ferrite layers corresponding to a stacking fault of the cationic sublattice, whereas the oxygen sublattice remains unchanged.

The films' stoichiometry was analyzed using *in situ* X-ray photoemission spectroscopy (XPS) with a Mg K_α source. The shapes of the Fe 2*p* and Ni 2*p* spectra are coherent with the Fe^{3+} and Ni^{2+} valence states and the expected 1/2 cationic (Ni/Fe) ratio is obtained by quantification of the peak intensities (Fig. 1(d)).

X-ray absorption spectroscopy (XAS) and X-ray magnetic circular dichroism (XMCD) experiments at the Fe and Ni $L_{2,3}$ edges were performed at room temperature under a magnetic field applied perpendicular to the surface to determine the occupancy of octahedral sites (labelled B) and tetrahedral sites (labelled A) in the spinel structure. The Fe $L_{2,3}$ edges XMCD spectrum (Fig. 2(a)), has been compared to calculated spectrum obtained by employing the ligand-field multiplet (LFM) model as described in Ref. 15 The best fit is obtained for a weighted sum of [44% Fe^{3+}(A) + 52% Fe^{3+}(B) + 4% Fe^{2+}(B)] proving that layers contain mainly Fe^{3+} cations, distributed almost equally between B and A sites. The Ni $L_{2,3}$ edges XMCD spectrum (Fig. 2(b)) is also qualitatively similar to that of Ni^{2+}(B).[16] Therefore, the cationic sites distribution in NFO thin films is consistent with the inverse structure predicted by theory[17] and measured by polarized Raman spectroscopy experiments.[18]

The magnetism of NFO(111) thin films has been studied by vibrating sample magnetometry (VSM). Fig. 3 shows the in-plane hysteresis loops of an ultrathin film after subtraction of the diamagnetic contribution from the substrate.[19] The

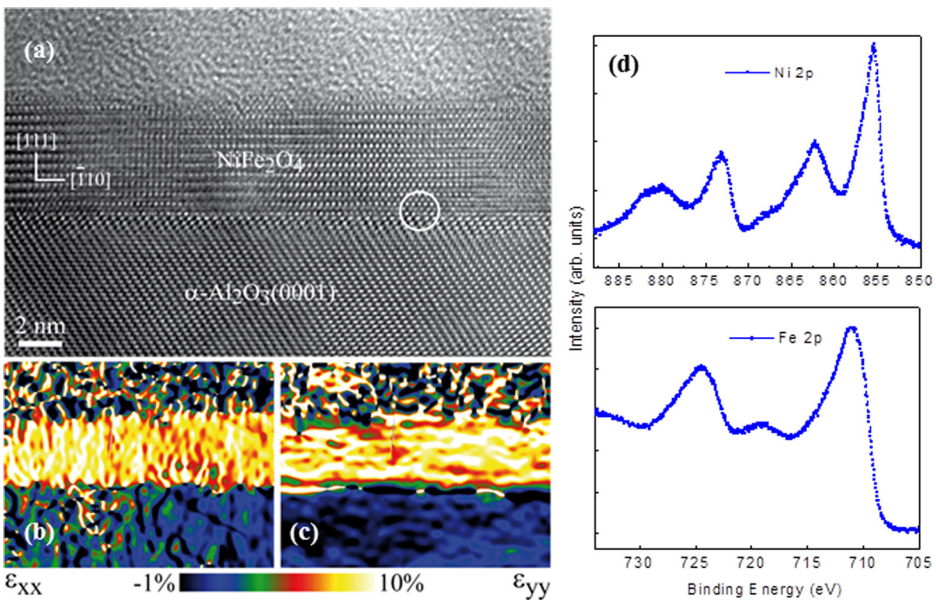

FIG. 1. (a) Cross-sectional HRTEM image of a α-Al_2O_3//$NiFe_2O_4$(111) (5 nm) film viewed along the [11-2] zone axis. The circle corresponds to the presence of a misfit dislocation. (b) and (c) Strain maps along the growth direction calculated from the HRTEM image using the GPA method for the (b) in-plane (ε_{xx}) and (c) out-of-plane (ε_{yy}) deformation. (d) Ni 2*p* and Fe 2*p* XPS spectra.

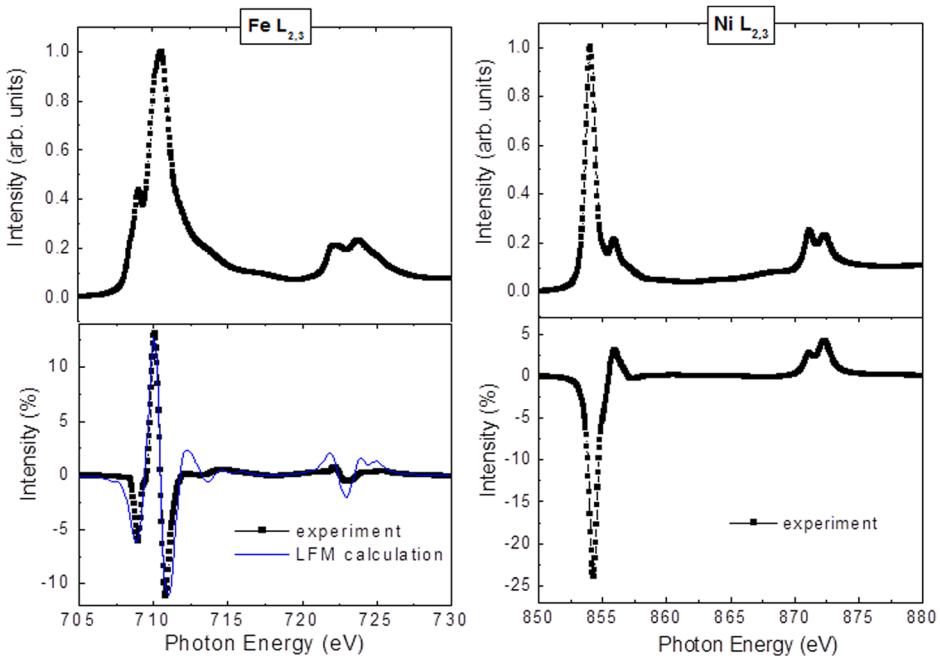

FIG. 2. Fe and Ni $L_{2,3}$ edges' XAS and XMCD spectra obtained for a α-Al_2O_3//Pt(111)/$NiFe_2O_4$(3 nm) film grown under $P_{O2} = 0.3$ Torr (T = 300 K, H = ±5 T) with the fit of the Fe $L_{2,3}$ edges' XMCD spectrum (blue line).

5 nm-thick film exhibits at T = 300 K an open hysteresis loop with a coercive field around 0.012 T, 18% of remanence and a net magnetization of 235 kA/m at high field, smaller than the magnetic moment of 2 μ_B per formula unit (i.e., 300 kA/m), calculated in the inverse spinel structure. At T = 10 K, the remanence increases up to 25% with a net magnetization around 260 kA/m and the coercive field increases to about 0.0365 T. The reduced values of remanent and high field magnetizations are consistent with the presence of APBs in ferrite thin films,[15,20–22] causing anti-ferromagnetic coupling between antiphase domain regions.

In order to examine the spin filtering efficiency of our NFO(111) tunnel barriers, Pt(111)/NFO(111)/γ-Al_2O_3(111)/Al tunnel junctions were constructed for Meservey-Tedrow experiments.[23] We choose to perform measurements on NFO(111) capped with γ-Al_2O_3(111) in order to reproduce the composite tunnel barrier used in future MTJs. In addition, the γ-Al_2O_3 allows preserving Al superconducting behaviour,

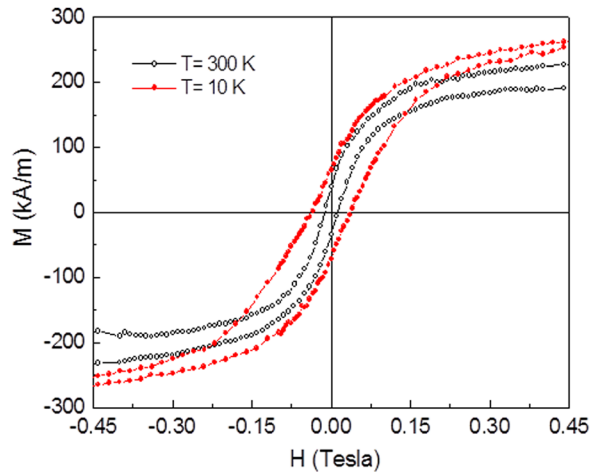

FIG. 3. In-plane magnetic hysteresis loops for an α-Al_2O_3//Pt/$NiFe_2O_4$(111) (5 nm) thin film at T = 300 K and 10 K.

while preventing the Al layer from reducing the surface of the ferrite, and it also serves to protect NFO from exposure to air. At first, we checked that the deposition of the γ-Al_2O_3(111) layer did not affect the physical properties of the NFO(111) tunnel barriers. Then, a 4.2 nm-thick Al layer (showing a superconducting critical temperature of 2.3 K) was deposited as cross strips, defining junctions with a lateral size of $500 \times 200\ \mu m^2$.

The tunneling dynamic conductance (dI/dV) curve measured at 0.45 K and zero magnetic field (Fig. 4(a)) for a $P_{O2} = 0.24$ Torr NFO barrier presents sharp symmetric peaks with a superconducting energy gap typical of Al. A Zeeman splitting of the superconductor (SC) quasiparticle density of states (DOS) with asymmetry is clearly observed when an in-plane magnetic field is applied proving that tunneling current is spin-polarized. By comparing the relative spin-up and spin-down peak heights, the asymmetry of the conductance peaks at H = 3.2 T corresponds to a spin-filter efficiency (P_{SF}) of 11% ± 1%. From the Maki-Fulde theory,[24] a fit of the DOS of the SC taking into account the Al spin-orbit scattering ($b = 0.04$), orbital depairing ($c = 0.1$), and Fermi liquid parameter ($e_0 = 0.8$) has been possible, confirming the value for P_{SF}. This result signs the first direct evidence of spin filtering in NFO.

The positive sign for P_{SF} is consistent with the positive TMR observed earlier in NFO(001)-based MTJs,[8,9] but in opposition with the negative P_{SF} expected theoretically for both the inverse or normal spinel structure.[17] The differences in the sign of P_{SF} between theory, Meservey-Tedrow or TMR measurements point out that both signs for the spin filtering are possible depending on additional factors, other than the DOS in the conduction band, such as the band alignment between the electrode and the ferrite or the specific wave-function symmetry inside the tunnel barrier.[25] A model based on the energy dependence of decay rates for spin-up and spin-down electrons[9] was proposed to explain the preferential tunneling of spin-up electrons and the positive sign for P_{SF} measured by TMR. In the case of our Meservey-Tedrow experiments, the band alignment in the epitaxial tunnel

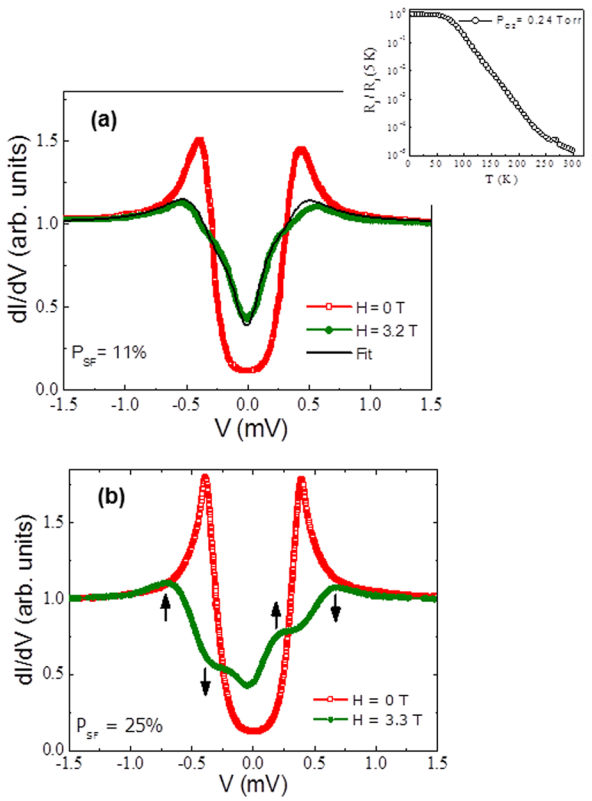

FIG. 4. (a) Spin-polarized tunneling in a α-Al_2O_3//Pt/$NiFe_2O_4$(4.1 nm)/γ-Al_2O_3(0.5 nm)/Al(4.2 nm) tunnel junction grown at $P_{O2} = 0.24$ Torr and measured at 0.45 K under zero and high magnetic field (H = 3.2 T). Inset: temperature-dependence of the junction resistance (R_J) normalized by the resistance value at 5 K. (b) Spin-polarized tunneling in a α-Al_2O_3//Pt/$NiFe_2O_4$(5 nm)/γ-Al_2O_3(1.5 nm)/Al(4.2 nm) junction [$P_{O2} = 0.44$ Torr] measured at 0.45 K under zero and 3.3 T.

junctions and the wave-function symmetry of the Al spin-analyzer could result in the preferential detection of the delocalized *sp* electrons with the spin-up symmetry, as it was mentioned in Meservey-Tedrow experiments performed on $CoFe_2O_4$[10] and $MnFe_2O_4$[12] spin-filters to explain the positive sign of the measured P_{SF}. In the low bias voltage regime, the bands in NFO are hardly deformed and the transport occurs via a direct tunneling mechanism. According to Mazin,[26] the spin-dependent DOS must be weighted by spin-dependent matrix elements governing the electrons transmission across the tunnel barrier. This revised definition of the tunneling SP may also potentially invert the sign of P_{SF}.

The amplitude of the measured SP is lower than the theory or the value deduced from TMR experiments ($P_{SF} = 22\%$ at 4 K),[8,9] probably due to the presence of defects states in NFO inducing parallel spin-independent conduction channels. In CFO(111) tunnel barriers, we have evidenced an increase of the spin-filter efficiency by decreasing the amount of oxygen vacancies.[10] The exponential increase of the junction resistance (R_J) with decreasing temperature (inset of Fig. 4(a)) is the mark of a thermally activated behavior with the presence of defects in our low-oxidized NFO barrier. The resistance-area product (R_JA) of the junction varied between 3 mΩ·cm^2 at 300 K and 9.7 Ω·cm^2 at 5 K. A significant improvement of the spin filtering efficiency has been achieved in more oxidized NFO barriers by decreasing the amount of oxygen vacancies, allowing to reach a R_JA of 35 Ω·cm^2 at 5 K and P_{SF} values up to 25% (for $P_{O2} = 0.44$ Torr, Fig. 4(b)). Nevertheless, the amplitude of P_{SF} remains lower than what could be expected, due to other defects affecting the spin-polarized tunneling. While cationic disorder can be discarded in our NFO barriers, the formation of APBs, evidenced by HRTEM, probably reduce the spin filtering efficiency by decreasing the conduction band exchange splitting and acting as preferential spin-independent conduction channels. The diminution of APBs[21,22] in ferrite ultrathin films appears thus particularly crucial in order to get higher SP.[6]

In summary, we have grown $NiFe_2O_4$(111) ultrathin films, showing high quality and full strain relaxation. The NFO layers present a cationic order in agreement with theory, with mainly Fe^{3+} and Ni^{2+} distributed in an inverse spinel structure. The magnetic properties are consistent with the expected behaviour in ferrite ultrathin films with defects such as APBs. We have demonstrated direct evidence of spin filtering by the Meservey-Tedrow technique with SP up to +25%. The unexpected positive sign for P_{SF} has revealed that the spin-polarized tunneling cannot just be explained by the asymmetry of the spin-dependent DOS; a full transport calculation for the entire device needs to be performed. The presence of defects in NFO tunnel barriers (in particular oxygen vacancies and APBs) has also been shown to affect the spin filtering efficiency. A fine tuning of the structure and chemistry of these oxide ultrathin layers is thus particularly critical for the generation of highly spin-polarized currents.

This work was supported by the PUF (Partner University Fund) Grand, NSF Grant No. DMR-1207469 and ONR Grant No. N00014-13-1-0301. We would like to acknowledge C. Deranlot for the growth of Pt(111) buffer layers and the METSA network for TEM characterizations. ESRF staff from ID08 beamline is thanked for his help during XAS and XMCD experiments.

[1]S. Yuasa, T. Nagahama, A. Fukushima, Y. Suzuki, and K. Ando, Nature Mater. **3**, 868 (2004).
[2]S. S. P. Parkin, C. Kaiser, A. Panchula, P. M. Rice, B. Hughes, M. Samant, and S. H. Yang, Nature Mater. **3**, 862 (2004).
[3]J. S. Moodera, T. S. Santos, and T. Nagahama, J. Phys.: Condens. Matter **19**, 165202 (2007).
[4]J. S. Moodera, R. Meservey, and X. Hao, Phys. Rev. Lett. **70**, 853 (1993).
[5]A. V. Ramos, M.-J. Guittet, J.-B. Moussy, R. Mattana, C. Deranlot, F. Petroff, and C. Gatel, Appl. Phys. Lett. **91**, 122107 (2007).
[6]S. Matzen, J.-B. Moussy, R. Mattana, K. Bouzehouane, C. Deranlot, and F. Petroff, Appl. Phys. Lett. **101**, 042409 (2012).
[7]J.-B. Moussy, J. Phys. D: Appl. Phys. **46**, 143001 (2013).
[8]U. Lüders, M. Bibes, K. Bouzehouane, E. Jacquet, J.-P. Contour, S. Fusil, J. Fontcuberta, A. Barthélémy, and A. Fert, Appl. Phys. Lett. **88**, 082505 (2006).
[9]U. Lüders, M. Bibes, S. Fusil, K. Bouzehouane, E. Jacquet, C. B. Sommers, J.-P. Contour, J.-F. Bobo, A. Barthélémy, A. Fert, and P. M. Levy, Phys. Rev. B **76**, 134412 (2007).
[10]A. V. Ramos, T. S. Santos, G. X. Miao, M.-J. Guittet, J.-B. Moussy, and J. S. Moodera, Phys. Rev. B. **78**, 180402(R) (2008).
[11]Y. K. Takahashi, S. Kasai, T. Furubayashi, S. Mitani, K. Inomata, and K. Hono, Appl. Phys. Lett. **96**, 072512 (2010).
[12]S. Matzen, J.-B. Moussy, G. X. Miao, and J. S. Moodera, Phys. Rev. B **87**, 184422 (2013).
[13]A. V. Ramos, S. Matzen, J.-B. Moussy, F. Ott, and M. Viret, Phys. Rev. B **79**, 014401 (2009).
[14]R. Datta, S. Kanuri, S. V. Karthik, D. Mazumbar, J. X. Ma, and A. Gupta, Appl. Phys. Lett. **97**, 071907 (2010).

[15]S. Matzen, J.-B. Moussy, R. Mattana, K. Bouzehouane, C. Deranlot, F. Petroff, J. C. Cezar, M.-A. Arrio, Ph. Sainctavit, C. Gatel, B. Warot-Fonrose, and Y. Zheng, Phys. Rev. B **83**, 184402 (2011).
[16]M. C. Richter, J. M. Mariot, O. Heckmann, L. Kjeldgaard, B. S. Mun, C. S. Fadley, U. Lüders, J.-F. Bobo, P. De Padova, A. T. Ibrahimi, and K. Hricovini, Eur. Phys. J.: Spec. Top. **169**, 175 (2009).
[17]Z. Szotek, W. M. Temmerman, D. Kodderitzsch, A. Svane, L. Petit, and H. Winter, Phys. Rev. B **74**, 174431 (2006).
[18]M. N. Iliev, D. Mazumbar, J. X. Ma, A. Gupta, F. Rigato, and J. Fontcuberta, Phys. Rev. B **83**, 014108 (2011).
[19]M. Foerster, J. M. Rebled, S. Estradé, F. Sanchez, F. Peiro, and J. Fontcuberta, Phys. Rev. B **84**, 144422 (2011).
[20]D. T. Margulies, F. T. Parker, M. L. Rudee, F. E. Spada, J. N. Chapman, P. R. Aitchison, and A. E. Berkowitz, Phys. Rev. Lett. **79**, 5162 (1997).
[21]S. Matzen, J.-B. Moussy, R. Mattana, F. Petroff, C. Gatel, B. Warot-Fonrose, J. C. Cezar, A. Barbier, M.-A. Arrio, and Ph. Sainctavit, Appl. Phys. Lett. **99**, 052514 (2011).
[22]C. Gatel, B. Warot-Fonrose, S. Matzen, and J.-B. Moussy, Appl. Phys. Lett. **103**, 092405 (2013).
[23]R. Meservey and P. M. Tedrow, Phys. Rep. **238**, 173 (1994).
[24]K. Maki, *Superconductivity* (Marcel Dekker, New York, 1969), Vol. 2.
[25]N. M. Caffrey, D. Fritsch, T. Archer, S. Sanvito, and C. Ederer, Phys. Rev. B **87**, 024419 (2013).
[26]I. I. Mazin, Phys. Rev. Lett. **83**, 1427 (1999).